ELSEVIER

S0032-3861(96)00465-X

Polymer Vol. 38 No. 1, pp. 59–78, 1997

0032-3861/97/$17.00 + 0.00

Compatibilizing effect of maleic anhydride functionalized SEBS triblock elastomer through a reaction induced phase formation in the blends of polyamide6 and polycarbonate: 2. Mechanical properties

S. Horiuchi*, N. Matchariyakult, K. Yase and T. Kitano
National Institute of Materials and Chemical Research, 1-1, Higashi, Tsukuba, Ibaraki, Japan

and H. K. Choi and Y. M. Lee
National Industrial Technology Institute, 2, Joogang-Dong, Kwachun, Kyungi-Do, Korea
(Received 5 March 1996)

The relationship between mechanical properties and phase morphology of blends of polyamide6 (PA6) and polycarbonate (PC) compatibilized with a maleic anhydride functionalized poly[styrene-b-(ethylene-*co*-butylene)-b-styrene] triblock copolymer (SEBS-gMA) were explored. The *in situ* chemical reaction between the maleic anhydride of SEBS and the amine end group of PA6 during melt mixing induces the encapsulation of SEBS-gMA on the PC domains in PA6 rich blends. Through this phase formation, the adhesion on the domain boundary between PA6 and PC are improved and thus mechanical properties are improved. The use of the combination of SEBS-gMA and unfunctionalized SEBS as compatibilizers has been found to provide remarkable improvement of mechanical properties in the PA6/PC blends. A transmission electron microscope (TEM) study has revealed that the encapsulation of SEBS around the PC domains becomes gradually incomplete by the use of both SEBS-gMA and unfunctionalized SEBS in the PA6 rich blends and at the same time the dispersed SEBS domains in the PA6 matrix enlarge with increasing the ratio of unfunctionalized SEBS to SEBS-gMA. In addition, the SEBS phase encapsulating the PC domains become thicker accompanying with the incompletion of the encapsulation. Although the encapsulation is incomplete, maximum impact strength and maximum strain at break in tensile test can be obtained when certain combinations of SEBS-gMA and SEBS are used. The observation of the domain boundary TEM has revealed that the thicker SEBS phase on the domain boundary contains the micro domain structure of SEBS, where the polystyrene phase forms a cylinder in a hexagonal arrangement in the poly(ethylene-*co*-butylene) matrix. Through this micro domain structure, SEBS is assumed to perform as a thermoplastic elastomer and toughen the domain boundary between PA6 and PC. Copyright © 1996 Elsevier Science Ltd.

(Keywords: compatibilization; polyamide6; polycarbonate)

INTRODUCTION

Polyamide6 (PA6) and polycarbonate (PC) both provide useful properties in a variety of applications and, therefore, have been widely used in various industrial fields. There however, are some negative aspects which are in some way symmetrical. That is, PA6 is strongly resistant to most solvents while PC is not; PC is insensitive to moisture and very stable against various weathering conditions while PA6 suffers greatly from moisture. Taking this into account, blends of PA6 and PC are expected to provide materials which complement the disadvantages of each polymer, overcoming the drawbacks, while maintaining the good properties. As reported by Gattiglia *et al.*[1–3], PA6 and PC are incompatible in the whole range of composition and temperature. PC does not interact well enough with PA6 to achieve an adequate dispersion of the components and the interface between these phases appears to be weak. As a result, the mechanical properties of simple blends of PA6 and PC are greatly inferior to those of the respective pure polymers. They also reported that the interchange reaction between PA6 and PC produces a block copolymer of PA6-PC during a long mixing and this enhances the compatibility of the interface between PA6 and PC[4]. However, the mechanical properties of the blends are still poor except for blends containing PA6 at 90 wt%. A solution has not yet been proposed to improve the mechanical properties of PA6/PC blends in the whole composition range.

There has been much interest recently in combining the attractive features of incompatible polymers by interfacial reaction: adding functionalized additives to form block or graft copolymers *in situ* during the blend

*To whom correspondence should be addressed
†Permanent address: Technology and Environmental Service, Rama 6 Road, Bangkok 10400, Thailand

processing. The blends of polyamide (PA)/styrene-acrylonitrile copolymer (SAN)[5], PA/acrylonitrile-butadiene-styrene (ABS)[6–8], PA/polypropylene (PP)[9–11], poly(butylene terephthalate) (PBT)/ABS[12] and PP/PBT[13] has been investigated in terms of the compatibilization by various functionalized polymers. We previously reported that the *in situ* reaction between amine end groups of PA6 and maleic anhydride functionalized SEBS induced the encapsulation of SEBS on PC domains in the PA6 matrix[14]. Through this phase formation, interfacial adhesion is improved and voids on the interface between PA6 and PC generated due to the difference of volume shrinkage of PA6 and PC disappear. On the other hand, in the PC rich blends (25/75 PA6/PC), SEBS-gMA is occluded inside the PA6 domains dispersed in the PC matrix and the occluded SEBS are partially formed domains and partially exist on the PA6 and PC interface inside the PA6 domains. In this case, interfacial adhesion between the PC matrix and PA6 domains are improved and then the voids on the interface, as observed in the incompatible blends, disappear. SEBS used in our work has its own micro domain structure which consists of a rod-shaped polystyrene (PS) phase arranged hexagonally in the poly(ethylene-butylene) (PEB) matrix. This structure is a thermoplastic elastomer in which the polystyrene rods work as physical cross-linking points below the PS glass transition temperature. The formation of the SEBS phase on the interface between PA6 and PC is expected to absorb the stress along the interface and, as a result, this leads to an improvement in mechanical properties, such as impact strength and tensile behaviour.

In this paper, we report on the mechanical properties of the PA6 and PC blends compatibilized with SEBS gMA and investigate the relationship to the phase morphology. The use of a combination of functionalized and unfunctionalized SEBS is also examined for this blend series. It is expected to be effective in improving toughness because it has been reported that the use of combination of SEBS-gMA and unfunctionalized SEBS is effective in toughening PA6 through controlling the dispersed SEBS size.

EXPERIMENTAL

Materials

All materials used in this work are supplied from commercial sources. Polyamide6 (PA6) is a hydrolytic poly(ϵ-caprolactam) (A1030BRF, Unichika Co.) with a number average molecular weight of 22 500 and melting flow rate of 4.3. The concentration of the amine end group was determined to be 5.0×10^{-5} mol g^{-1} by the titration. Bisphenol-A polycarbonate (PC) was supplied by Teijin Chemical Co. Ltd of which product name is Panlite L-1250Y. These two polymers were dried at 80°C for at least 12 h in a vacuum oven to remove sorbed water before processing. The triblock copolymer of poly[styrene-b-(ethylene-*co*-butylene)-b-styrene] (SEBS) was incorporated into the PA6 and PC blends for compatibilizing the system. This copolymer has styrene end blocks and a hydrogenated butadiene midblock resembling an ethylene/butylene copolymer. The SEBS was functionalized with 2% (wt) maleic anhydride onto the hydrocarbon chains, designated SEBS-gMA (Kraton 1901) supplied by Shell, with a molecular weigh of 20 000 and styrene content of 29% (wt). Unfunctionalized SEBS used was Kraton 1652 with the same molecular weight and styrene contents as Kraton 1901.

Blending procedures

PA6 and PC were mixed using the compact mixing machine developed in our laboratory. The details of this machine was described in our previous paper[14] and the blending conditions were also the same as reported previously[14]. That is, 10 g total PA6 and PC with varying levels of SEBS-gMA and/or SEBS were put into the mixing room simultaneously and were mixed at a rotation speed of 80 rpm at 260°C for 10 min. A blended sample was then injected into a mould placed just below the machine. The moulded sheet was 3 mm in thickness. The composition of PA6/PC was held at 25/75, 50/50 and 75/25, while the amount of added SEBS-gMA and/or SEBS was varied from 5 phr (5 g against 100 g of the total amount of PA6 and PC) to 20 phr.

Testing of mechanical properties

To characterize the mechanical properties of the blends, the impact strength on notched samples and stress–strain measurements were carried out for the moulded specimens. The izod impact strength on notched samples was measured using a Toyoseiki Universal Impact tester, according to ASTM D256. Stress–strain measurements were carried out using a Shimadzu Autograph, AG-10TB, in accordance with ASTM D638 using a crosshead speed of 20 mm min^{-1}. All tests were carried out at constant temperature and humidity of 23°C, 60%. All specimens were dried overnight at 100°C and stored in a desiccator,. The reported values are the average of at least five specimens.

Transmission electron microscopy

Morphological studies were carried out by transmission electron microscopy (TEM). Sections were microtomed from moulded samples perpendicular to the flow direction, and afterward stained with ruthenium tetraoxide (RuO_4). The staining agents were used as aqueous solutions of 0.5 wt% RuO_4. Electron spectroscopic images (ESI) were taken to obtain the images with maximum resolution using a Zeiss CEN 902 at an accelerating voltage of 80 kV which attaches an integrated electron energy loss spectrometer for electron energy loss spectroscopy (EELS). We have demonstrated the usefulness of ESI for morphological study in polymer blends previously[14]. Detailed descriptions of ESI and EELS have appeared in the literature[15,16]. Images were recorded on an imaging plate (IP) and processing of the obtained images was carried out using FDL5000 (Fuji Photofilm Film Co., Ltd). A semi-automatic digital image analysis technique was employed to determine the size of dispersed domains from TEM photographs using an IBAS image processor. More than 200 particles were counted and the diameter assigned to each particle was determined as that of a circle with equivalent area.

Scanning electron microscopy

Fracture surfaces of blend materials were observed with a scanning electron microscope, Topcon DS-720, at an accelerating voltage of 15 kV. The specimens fractured after tensile testing were coated with gold to make them electrically conducting.

Table 1 Mechanical properties of the PC/SEBS-gMA, PA6/SEBS-gMA and PA6/SEBS-gMA/SEBS blends

Formulation	Notched izod impact ($J\,m^{-1}$)	Tensile modulus (GPa)	Yield		Break	
			Stress (MPa)	Strain (%)	Stress (MPa)	Strain (%)
PC/SEBS-gMA						
100/0	645.6	2.04	64.3	3.5	63.4	112.8
100/5	627.2	1.71	58.6	3.8	59.3	104.2
100/10	697.2	1.55	44.4	4.0	52.7	84.2
100/15	532.6	1.37	43.0	5.6	38.1	34.9
PA6/SEBS-gMA						
100/0	78.3	2.37	75.3	3.7	85.0	166.7
100/55	132.7	1.81	57.9	4.5	52.4	197.4
100/10	259.6	1.72	46.5	5.0	46.2	170.7
100/15	817.3	1.59	43.5	5.5	45.6	205.0
75/5	NT	2.01	58.3	4.7	44.2	205.0
75/10	NT	1.76	54.5	5.3	46.8	142.0
75/15	NT	1.57	48.5	5.9	43.4	200.0
25/10	NT	1.16	38.1	6.7	38.8	242.7
25/15	NT	1.03	31.8	7.2	45.1	250.0
PA6/SEBS-gMA/SEBS						
75/20/0	576.6	1.53	45.7	6.50	47.9	182.9
75/15/5	639.2	NT	NT	NT	NT	NT
75/10/10	588.3	NT	NT	NT	NT	NT
75/5/15	120.6	NT	NT	NT	NT	NT
75/0/20	64.9	NT	NT	NT	NT	NT

NT: Not tested

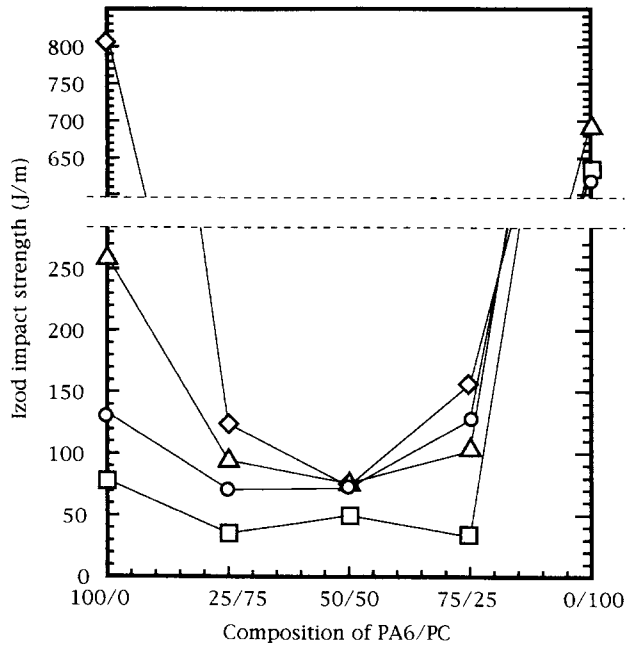

Figure 1 Notched izod impact strength of PA6/PC blends compatibilized with SEBS-gMA as a function of PC weight fraction: uncompatibilized blends (□); 5 phr (○), 10 phr (△) and 15 phr (◇) of SEBS-gMA added

RESULTS AND DISCUSSION

Izod impact strength of the PA6 and PC blends compatibilized with SEBS-gMA

Gattiglia *et al.* have reported stress–strain behaviour and izod impact strength of various compositions of

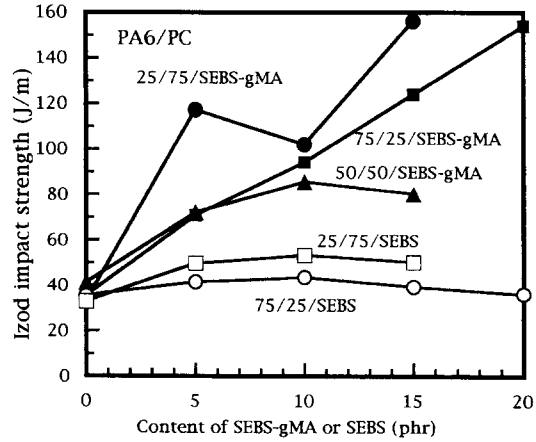

Figure 2 Notched izod impact strength of PA6/PC blends with SEBS-gMA or SEBS as a function of the content of SEBS-gMA or SEBS: (●) 25/75, (▲) 50/50 and (■) 75/25 PA6/PC blends with SEBS-gMA; 25/75 (□) and 75/25 (○) PA6/PC blends with SEBS

PA6/PC blends[2]. They reported that in all composition ranges the blends show much poorer mechanical properties than those of the respective pure polymers. In this study, to evaluate the effect of SEBS-gMA as a compatibilizer, we fixed the composition of PA6/PC at 75/25, 50/50 and 25/75 and varied the amount of SEBS-gMA.

Blends of PA6 and PC with varying levels of SEBS-gMA were prepared using the procedures outlined earlier. The notched izod impact strength for all blends are shown in *Tables 1* and *2*. *Figure 1* shows the notched izod impact strength for blends of PA6/PC with various amounts of SEBS-gMA as a function of the composition

Table 2 Mechanical properties of the PA6/PC/SEBS-gMA and PA6/PC/SEBS-gMA/SEBS blends

Formulation	Notched izod impact ($J\,m^{-1}$)	Tensile modulus (GPa)	Yield		Break	
			Stress (MPa)	Strain (%)	Stress (MPa)	Strain (%)
PA6/PC/SEBS-gMA/SEBS						
75/25/0/0	35.4	2.10	NI	NI	65.2	4.4
75/25/5/0	70.8	1.94	56.6	4.6	44.1	25.0
75/25/0/5	41.4	1.90	NI	NI	58.1	6.0
75/25/10/0	94.4	2.04	48.0	3.8	35.9	31.3
75/25/8/2	115.4	1.75	42.9	3.7	35.2	42.6
75/25/6/4	119.6	NT	NT	NT	NT	NT
75/25/5/5	NT	1.83	45.0	3.8	39.9	177.7
75/25/4/6	125.3	NT	NT	NT	NT	NT
75/25/2/8	110.2	1.85	43.9	3.6	36.1	27.3
75/25/0/10	43.5	1.85	52.7	5.2	42.5	5.8
75/25/15/0	124.0	1.58	42.1	4.4	40.8	56.0
75/25/0/15	39.3	1.80	46.0	3.8	40.8	6.8
75/25/20/0	154.1	1.50	41.3	4.7	33.9	59.1
75/25/19/1	607.2	NT	NT	NT	NT	NT
75/25/17/3	681.1	NT	NT	NT	NT	NT
75/25/15/5	692.0	1.45	35.4	5.8	33.4	250.0
75/25/13/7	684.3	NT	NT	NT	NT	NT
75/25/10/10	640.5	1.55	35.8	4.9	34.7	235.1
75/25/5/15	560.7	1.52	34.3	4.7	38.5	242.7
75/25/2/18	145.3	NT	NT	NT	NT	NT
75/25/0/20	40.0	1.75	49.6	4.0	39.6	8.7
50/50/0/0	41.2	1.96	NI	NI	41.5	2.4
50/50/5/0	72.1	1.77	46.6	5.1	38.3	34.6
50/50/10/0	85.6	1.56	43.6	6.7	69.9	23.5
50/50/15/0	80.2	1.38	41.5	7.0	37.0	33.5
25/75/0/0	32.9	1.75	NI	NI	47.7	3.8
25/75/5/0	117.3	1.38	41.9	5.6	40.9	6.5
25/75/0/5	49.7	1.57	NI	NI	48.8	4.7
25/75/10/0	102.1	1.16	37.7	5.4	35.5	13.3
25/75/8/2	121.2	NT	NT	NT	NT	NT
25/75/5/5	141.8	NT	NT	NT	NT	NT
25/75/2/8	107.5	NT	NT	NT	NT	NT
25/75/0/10	53.4	1.44	NI	NI	41.1	4.2
25/75/15/0	156.1	0.98	34.6	5.9	30.6	22.4
25/75/0/15	50.2	1.26	NI	NI	39.6	5.2

NI: Not identified; NT: not tested

of PA6/PC. The uncompatibilized blends show impact strength greatly inferior to the respective pure polymers. In particular the outstanding impact strength of PC is drastically reduced from approximately 700 to $50\,J\,m^{-1}$ by the addition of PA6. This drastic reduction of impact strength demonstrates that the PA6/PC blends are incompatible in the full range of compositions. As shown previously[14], the uncompatibilized blends are characterized by a biphasic structure in which one component is dispersed in the other one and voids on the domain boundary are generated due to the weak interfacial adhesion. Pure PA6, on the other hand, is rather brittle, having an impact strength of $78.3\,J\,m^{-1}$. But the addition of SEBS-gMA increases the impact strength remarkably, up to about 10 times. The impact strength of PA6/PC blends are increased by the addition of SEBS-gMA, but the effect of this addition is not so remarkable as that for pure PA6. Although the PA6/PC blends compatibilized with SEBS-gMA show a lower impact strength than that of pure PC and that of the binary blends of PA6/SEBS-gMA, it is obvious, as shown in *Figure 2*, that the impact strength is increased with an increasing amount of SEBS-gMA in all the PA6/PC composition range, while the addition of unfunctionalized SEBS provides no contribution to the improvement of impact strength. *Figures 3a* and *b* show TEM photographs of PA6 rich (75/25) and PC rich (25/75) blends compatibilized with 5 phr SEBS-gMA, respectively, where the polystyrene blocks of SEBS are stained with RuO_4. In the blends of 75/25, PA6 forms a matrix,

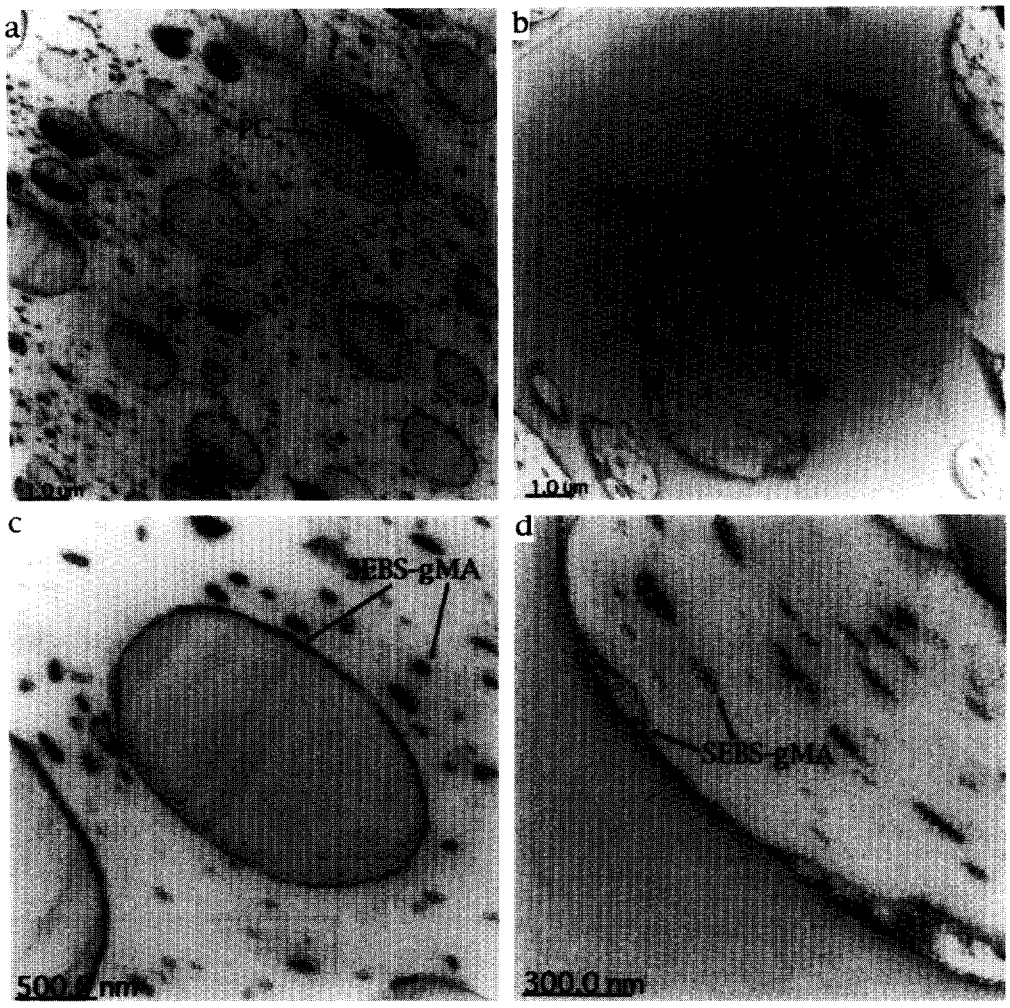

Figure 3 TEM photograph of the blend of (a) 75/25/5 and (b) 25/75/5 PA6/PC/SEBS-gMA. (c) and (d) are higher magnification views of (a) and (b), respectively

and SEBS-gMA and PC domains are dispersed in the PA6 matrix, while SEBS-gMA is occluded in PA6 domains in the 25/75 PA6/PC blend. As shown in the higher magnification view in *Figure 3c* and *d*, SEBS-gMA encapsulates PC domains in PA6 rich blends, and in PC rich blends SEBS-gMA exists on the domain boundary between PA6 and PC. The detailed morphological analysis reported in the previous paper[14] has revealed that *in situ* reaction during mixing between the amine end groups of PA6 and maleic anhydride grafted on SEBS occurred and, as a result, the fine dispersion of SEBS in PA6 phase can be achieved in the blends of 75/25 and 50/50 PA6/PC blends and, moreover, the encapsulation of SEBS on PC domains is induced in PA6 matrix. The size of the dispersed SEBS-gMA domains in the PA6 matrix obtained from image analysis of TEM photographs is almost constant both in the ternary blends of PA6/PC/SEBS-gMA and in the binary blends of PA6/SEBS-gMA, as summarized in *Table 3*. SEBS-gMA is known to work as an impact modifier in the blends with polyamide[17–22] through the chemical reaction at the interface. With respect to the morphological features of blends of 75/25 with SEBS-gMA as shown in *Figure 3*, it is speculated that SEBS-gMA works as an impact modifier for the PA6 matrix and at the same time works as a coupling agent for the adhesion of PC domains to the PA6 matrix. Compared to the dramatic improvement of impact strength achieved in the binary blends of PA6/SEBS-gMA, the impact strength of the ternary blends PA6/PC/SEBS-gMA are still unsatisfied. The reason for that is assumed to be that the PC domains in the PA6 matrix are too large and cannot be reduced by the addition of SEBS-gMA as shown in *Table 3*. In addition, the interfacial adhesion between the PC domains and the PA6 matrix may be insufficient to offer high impact strength.

PC rich blends also show an improvement in impact strength by the addition of SEBS-gMA as shown in *Figure 2*. The addition of SEBS-gMA is more effective than in the PA6 rich blends. As mentioned in our previous paper[14], the occluded SEBS-gMA in the PA6 domains are dispersed as domains and also exist on the domain boundary between PA6 and PC. The role of SEBS-gMA in PC rich blends may be different from that in the PA6 rich blends, because SBS-gMA cannot work as the impact modifier for PC matrix as shown in *Table 1*. Therefore PA6 domains with occluded SEBS-gMA are themselves assumed to contribute to the increase of the impact strength in the PC rich blends.

The effect of the combination of SEBS-gMA and SEBS to the impact strength of PA6/PC blends

Paul *et al.* have reported that when certain combinations of SEBS-gMA and SEBS are added to nylon6,

Table 3 Average diameter and related parameters for the PC and SEBS domains dispersed in the PA6 matrix obtained from TEM photographs

Formulation	PC domain			SEBS domain		
	Number average diameter (μm)	Standard deviation (μm)	Median value (μm)	Number average diameter (nm)	Standard deviation (nm)	Median value (nm)
PA6/SEBS-gMA/SEBS						
75/20/0	—	—	—	138	59	133
75/15/5	—	—	—	163	111	137
75/10/10	—	—	—	238	195	190
75/5/15	—	—	—	335	241	271
PA6/PC/SEBS-gMA/SEBS						
75/25/5/0	1.95	1.12	1.73	140	61	148
75/25/10/0	1.50	1.31	1.33	145	53	148
75/25/8/2	1.96	1.18	1.55	226	75	215
75/25/5/5	2.06	1.23	1.71	262	133	231
75/25/2/8	2.12	1.46	1.80	314	188	261
75/25/15/0	1.60	1.20	1.55	130	40	125
75/25/20/0	1.76	1.13	1.46	134	55	131
75/25/19/1	1.66	1.20	1.36	180	71	167
75/25/17/3	1.82	1.01	1.61	216	102	195
75/25/15/5	1.70	1.00	1.42	195	90	171
75/25/13/7	1.87	1.08	1.59	215	92	200
75/25/10/10	2.13	1.31	1.71	242	154	195
75/25/5/15	1.89	1.00	1.59	261	213	194
75/25/2/18	2.13	1.22	1.81	322	238	265
75/25/0/20	1.83	1.70	1.35	—	—	—

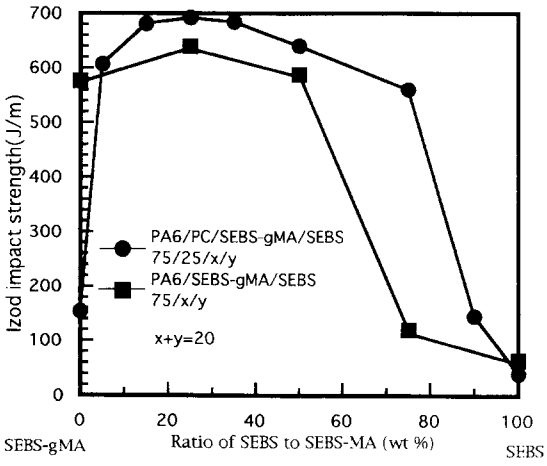

Figure 4 Notched izod impact strength of 75/25 PA6/PC blends and PA6 blends, in which the ratio of total amount of SEBS to PA6 is 20/75, as a function of the ratio of SEBS-gMA to unfunctionalized SEBS: (●) PA6/PC blends; (■) PA6 blends

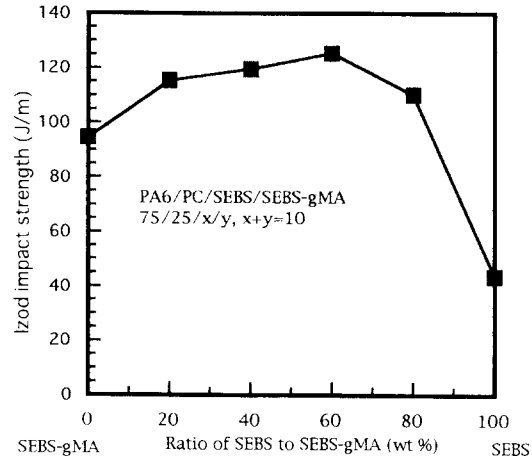

Figure 5 Notched izod impact strength of 75/25 PA6/PC blends compatibilized with a combination of SEBS-gMA and SEBS. The total amount of SEBS-gMA and SEBS is 10 phr and the ratio of SEBS-gMA to SEBS is varied

super-tough blends are obtained[17]. They reported that SEBS-gMA and SEBS coexist in the same particles and varying the ratio of functionalized and unfunctionalized SEBS is an effective way of controlling particle size and hence blend properties. This result encouraged us to investigate the effect of the combination of SEBS-gMA and SEBS on the compatibilization of PA6/PC blends. *Table 2* includes the izod impact strength of 75/25 and 25/75 PA6/PC blends containing both SEBS-gMA and SEBS at varying levels. As shown in *Figure 4*, the dramatic improvement of impact strength can be achieved in 75/25 PA6/PC blends when the total amount of added SEBS-gMA and SEBS are held constant at 20 phr and the ratio of SEBS-gMA to SEBS are varied. In particular, it is interesting to note that the replacement of only 1 phr of SEBS-gMA to unfunctionalized SEBS leads to a remarkable improvement of impact strength from 130 to 600 J m^{-1}. As shown in *Figure 5*, this trend is also detectable in the blends of PA6/PC 75/25 containing 10 phr total amount of SEBS-gMA and SEBS, although the drastic enhancement of impact strength cannot be achieved. The impact strength of PA6 toughened with a combination of SEBS-gMA and SEBS, in which the ratio of the total amount of SEBS-gMA and SEBS to PA6 is the same as that in the blends of PA6/PC, is also plotted in *Figure 4*. This shows

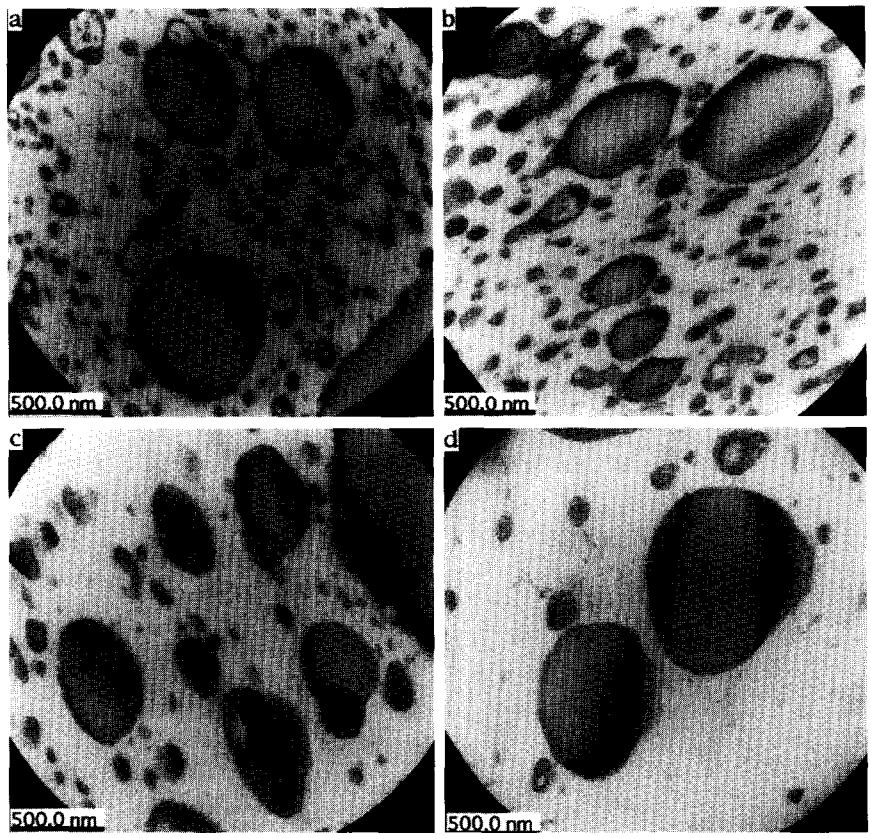

Figure 6 TEM photographs of PA6/PC/SEBS-gMA/SEBS blends at the same magnification where SEBS domains are stained with RuO_4: (a) 75/25/20/0, (b) 75/25/19/1, (c) 75/25/10/10 and (d) 75/25/5/15

that PA6 can be toughened successfully by the addition of both SEBS-gMA and SEBS. The comparison of these two blend series indicates that the blends of PA6/PC compatibilized with certain combinations of SEBS-gMA and SEBS exhibit higher impact strength than those of PA6 toughened with a combination of SEBS-gMA and SEBS. Now, we note that the impact strength of the ternary blends of PA6/SEBS-gMA/SEBS obtained in our study is somewhat different from those reported by Paul *et al.*[17]. They reported that the maximum impact strength was obtained when the ratio of SEBS-gMA to SEBS was *ca* 1–4 in the blends containing a total SEBS both functionalized and unfunctionalized at 20 wt%. In our case, on the contrary, the maximum strength is obtained in the blends containing both SEBS-gMA and SEBS in the ratio of 4–1. We believe that the origin of this difference may lie in the method of sample preparation. They used a single or twin extruder, while we used a miniature moulding system. For reactive blend systems, the final morphology strongly depends on the blend process. That is, more intense mixing or a higher shear rate should lead to a reduction in the dispersed domain size[22]. As a result, the size of the SEBS domain of our samples may be different from that of the previous workers.

To understand the effect caused by the use of both functionalized and unfunctionalized SEBs, we characterized morphological variations obtained by varying the ratio of SEBS-gMA to SEBS. *Figure 6* shows the TEM photographs of 75/25/20/0, 75/25/19/1, 75/25/10/10 and 75/25/5/15 PA6/PC/SEBS-gMA/SEBS blends at the same magnification, where RuO_4 is used for staining of polystyrene domains in SEBS. These blends involve the four components but are composed of three phases, which means that SEBS-gMA and SEBS coexist in the same domains. *Figure 7* shows a higher magnification view focused on the SEBS domains in the blend series. From the simple visual inspection of these photographs, it is revealed that, with an increase of the ratio of unfunctionalized SEBS to SEBS-gMA, the size of the SEBS domains dispersed in PA6 matrix is increased, while the size of PC domains is relatively constant. Interestingly, as shown in *Figure 8*, the encapsulation of SEBS on the PC domains gradually become incomplete with increase of the ratio of unfunctionalized SEBS to SEBS-gMA and, finally, the attached formation of SEBS onto a PC domain is obtained by the use of 20 phr of unfunctionalized SEBS alone. Taking into consideration the morphological variations mentioned above by varying the ratio of SEBS-gMA to SEBS and keeping the total amount held constant at 20 phr, three factors which would reflect the imapct strength could be changed in the phase formation of them. One is the size of SEBS domains dispersed in the PA6 matrix, one is the size of PC domains and the other is the interfacial situation between the PC domains and PA6 matrix. For quantification of particle size distribution, digital image analysis was carried out with the TEM photographs for the series of 75/25 PA6/PC blends compatibilized with 20 phr total of SEBS-gMA and SEBS. When image analysis is carried out using TEM photographs, it has to be remembered that the particles are rarely cut through their equators and therefore the values obtained are smaller and more broadly distributed in size than they

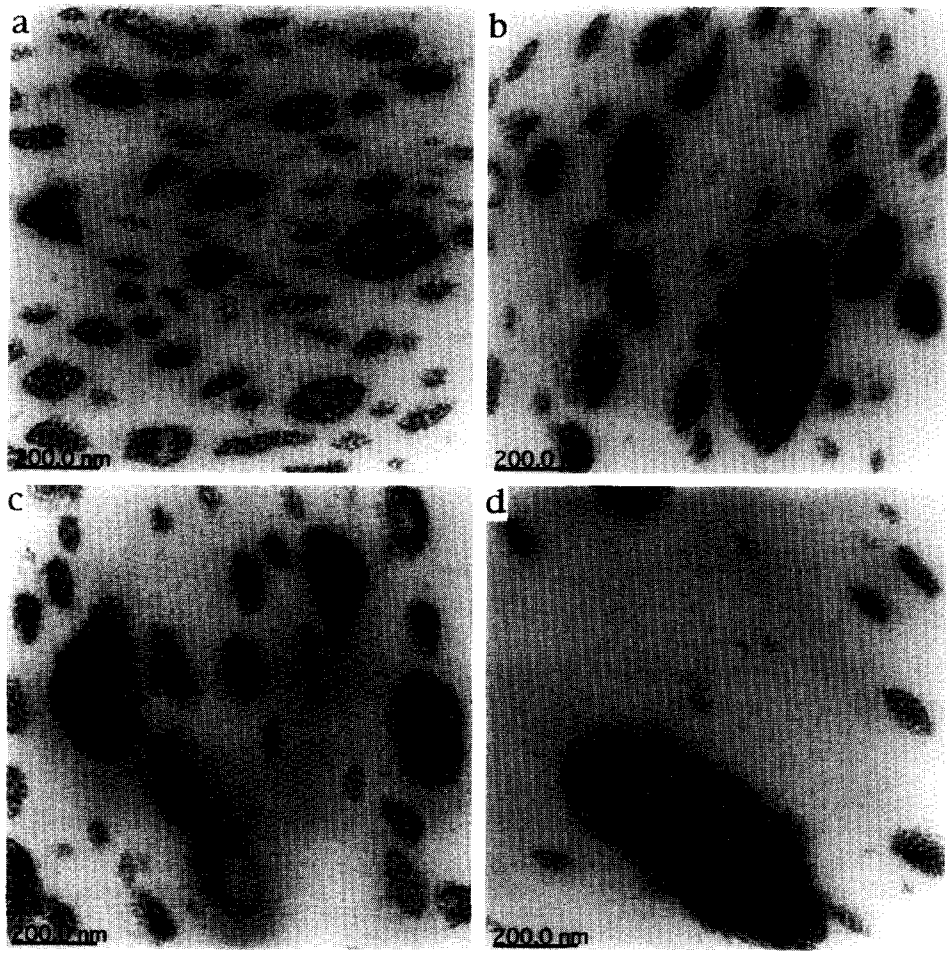

Figure 7 TEM photographs showing SEBS domains at the same magnification in PA6/PC/SEBS-gMA/SEBS blends: (a) 75/25/20/0, (b) 75/25/15/5, (c) 75/25/10/10 and (d) 75/25/5/15

really are. In this study, we did not apply any methods to correct this effect because it is not necessarily required for the relative size comparison. Particle size information from the TEM photographs is summarized in *Table 3*. *Figure 9a* shows the number-average diameter of the SEBS domains dispersed in the PA6 matrix as a function of the ratio of SEBS-gMA to SEBS in the 75/25 PA6/PC blends in which the total amounts of SEBS-gMA and SEBS are fixed at 20 phr. This reveals that with an increase of the ratio of unfunctionalized SEBS to functionalized, the size of SEBS domains is increased and, especially, by the replacement of 1 phr SEBS-gMA to SEBS a strong increase in average diameter is shown. On the other hand, the PC domains show no drastic change in size and are around 2 μm as shown in *Figure 9b*. To confirm whether SEBS-gMA and SEBS reside in the same domains uniformly or exist separately, the distribution of the particle size is checked. If the two components exist separately in two populations, there should be a strong bimodality in the particle size distribution owing to the large difference in sizes for SEBS and SEBS-gMA individually. Conversely, a unimodal distribution would indicate the coexistence of the two polymers. *Figure 10* shows histograms for number of particles against specified ranges of size obtained by counting particles in the PA6/PC/SEBS-gMA/SEBS blends and in the ternary PA6/SEBS-gMA/SEBS blends. In both blend series, the histograms for the blends containing unfunctionalized SEBS at a higher level show bimodality in both cases, while none of the other samples show evidence for such bimodality, although the particle size distributions are broad and have a significant tail. The average diameters obtained in this study show overall larger value than those reported by Paul *et al.* owing to the difference of the way of mixing. These particle size distributions, however, show a qualitatively similar trend to that reported by them. These results support the evidence that the effect of the use of the combination of functionalized and unfunctionalized SEBS on controlling the size of particles is the same in both blends of PA6/PC, and PA6 alone.

Paul *et al.* have reported that for toughening PA6 by controlling the size of SEBS domains, using both SEBS-gMA and SEBS, there is not only an upper size limit on the particle size but also a lower size limit. *Figure 11* shows the relationship between SEBS domain size and impact strength in the blends of PA6/PC compatibilized with the combination of SEBS-gMA/SEBS, and in the blends of PA6 toughened with SEBS-gMA/SEBS. Both blend series contain total amount of SEBS-gMA and unfunctionalized SEBS at the same ratio to PA6 at 20–75 by weight. This result indicates that SEBS-gMA alone forms domains that are too small for effective toughening. With an increase of the ratio of unfunctionalized

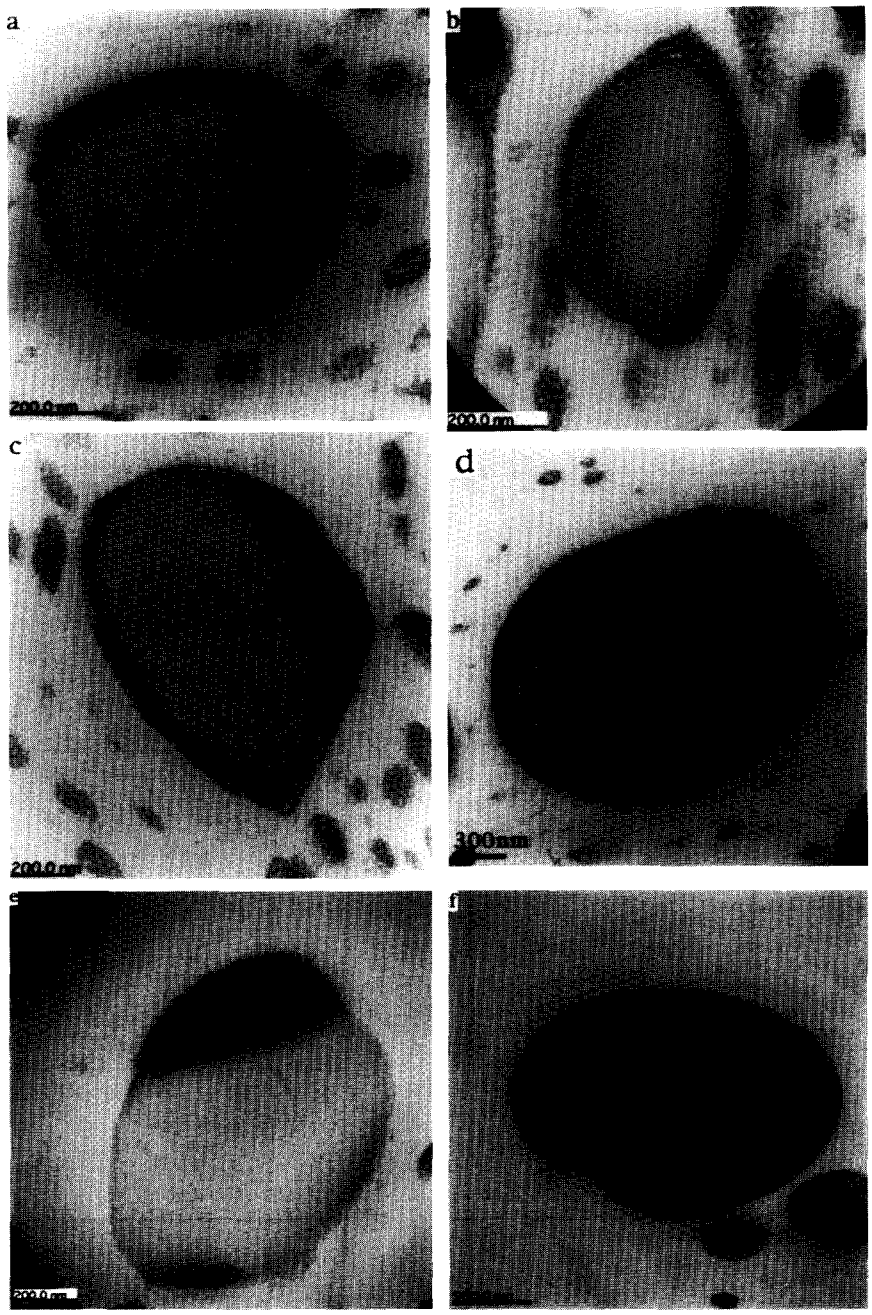

Figure 8 TEM photographs showing the SEBS phase encapsulating the PC domains in PA6/PC/SEBS-gMA/SEBS blends: (a) 75/25/20/0, (b) 75/25/19/1, (c) 75/25/10/10, (d) 75/25/5/15, (e) 75/25/2/18 and (f) 75/25/0/20

SEBS, the domain size can go beyond the critical lower limit size and maximum impact strength can be achieved. These two blend series, however, show different behaviours in the relationship between the impact strength and the SEBS domain size in the blends containing SEBS-gMA at higher ratio. Although the dispersed domain size is equivalent in the blend of 75/25 compatibilized with 20 phr of SEBS-gMA and in the binary blend of 75/20 PA6/SEBS-gMA (*ca* 130 nm), the impact strength obtained in the case of the PA6/PC blend is much lower than that of the PA6/SEBS blend and, moreover, the dramatic increase of impact strength by the replacement of 1 phr of SEBS-gMA to unfunctionalized SEBS is found only in the PA6/PC blend. These results suggest that the reason for the drastic improvement of impact strength by the use of combination of SEBS-gMA and SEBS in the PA6/PC blends cannot be explained only in terms of the size variation of SEBS domains dispersed in the PA6 matrix. As mentioned earlier, the size of PC domains are almost constant at around 2 μm with changing the ratio of SEBS-gMA to SEBS. The interfacial situation on the domain boundary between PA6 and PC, therefore, has to be taken into consideration. *Figure 12* shows the interfacial situation between the PA6 and PC domain where PS domains in SEBS are stained with RuO_4. In the 75/25 PA6/PC blend with SEBS-gMA alone, it is detectable in the TEM photograph in *Figure 12a* that the PS domain of SEBS contacts the PC domain for about 6 nm thickness and, due to the chemical reaction on the interface between PA6 and SEBS-gMA, the microdomain structure of SEBS is disordered at the interface between PA6 and

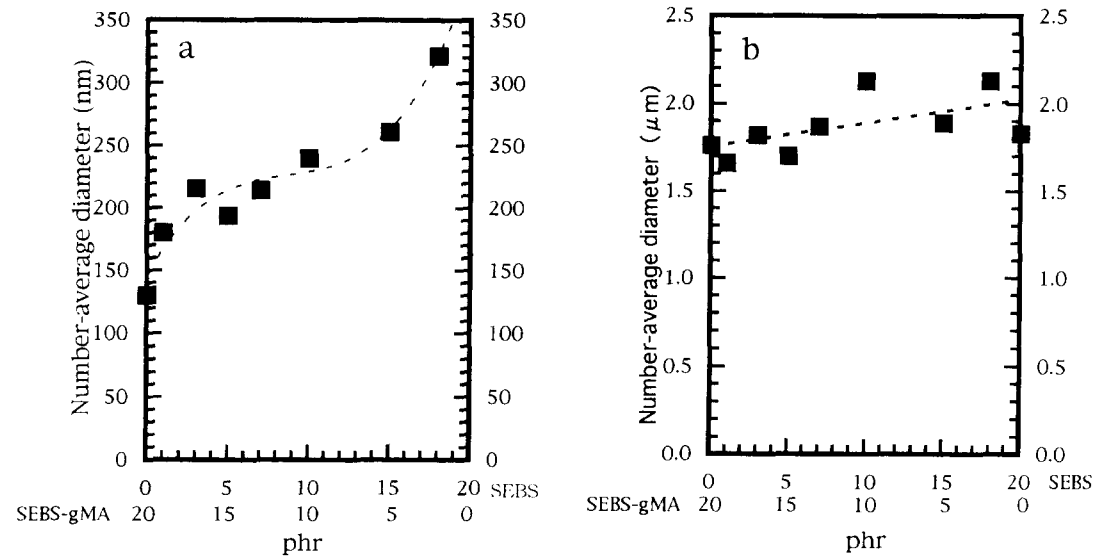

Figure 9 The number-average particle diameter of (a) SEBS domains and (b) PC domains dispersed in the PA6 in 75/25 PA6/PC blends compatibilized with the SEBS-gMA and SEBS combination as a function of the ratio of SEBS-gMA to SEBS. The total amount of SEBS-gMA and SBS is 20 phr and the ratio of SEBS-gMA to SEBS is varied

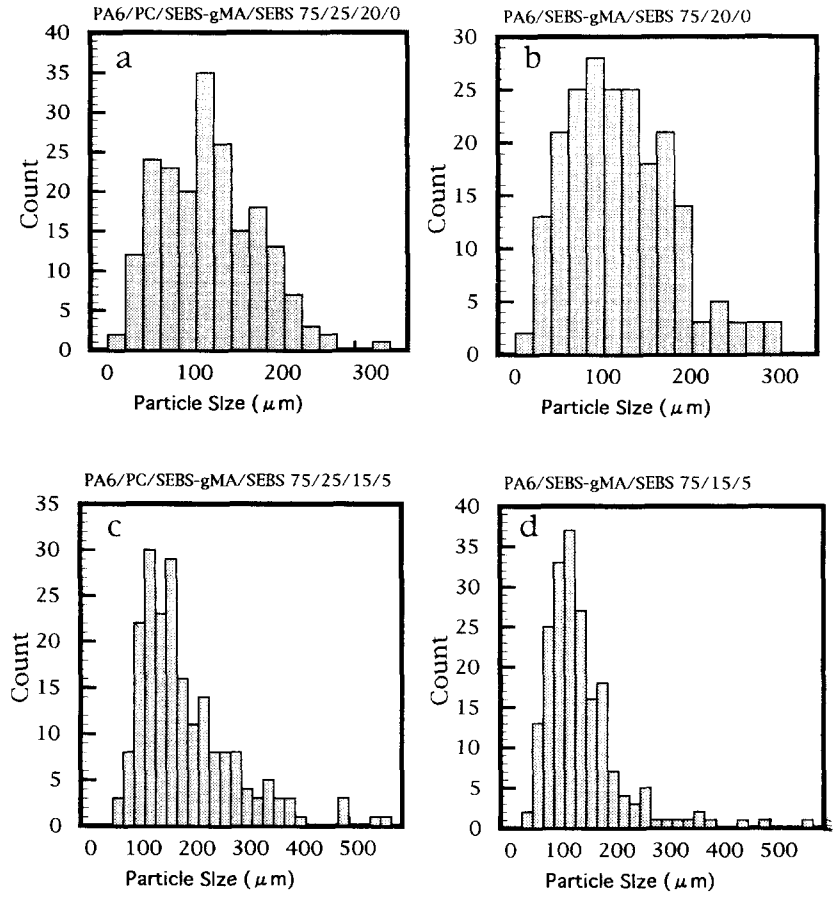

Figure 10 Histograms showing the distribution of SEBS domain size in the 75/25 PA6/PC blends and in PA6 blends with a combination of SEBS-gMA and SEBS. The formulations are denoted on the upper side of each of the histograms

SEBS-gMA. The encapsulation of SEBS-gMA is so thin that no original SEBS microdomain structure appears on the domain boundary. On the other hand, *Figure 12b* clearly shows that the original microdomain structure of SEBS, in which PS forms cylinders arranged hexagonally in the PEB matrix, remains in between the two different types of interfaces in the 75/25/19/1 blend, although the encapsulation of SEBS-gMA on PC domains is incomplete. With an increase in the ratio of unfunctionalized SEBS, the SEBS phase on the PC domains become thicker and the original microdomain structure of PS domains appear in a larger area, as shown in *Figure 12c*.

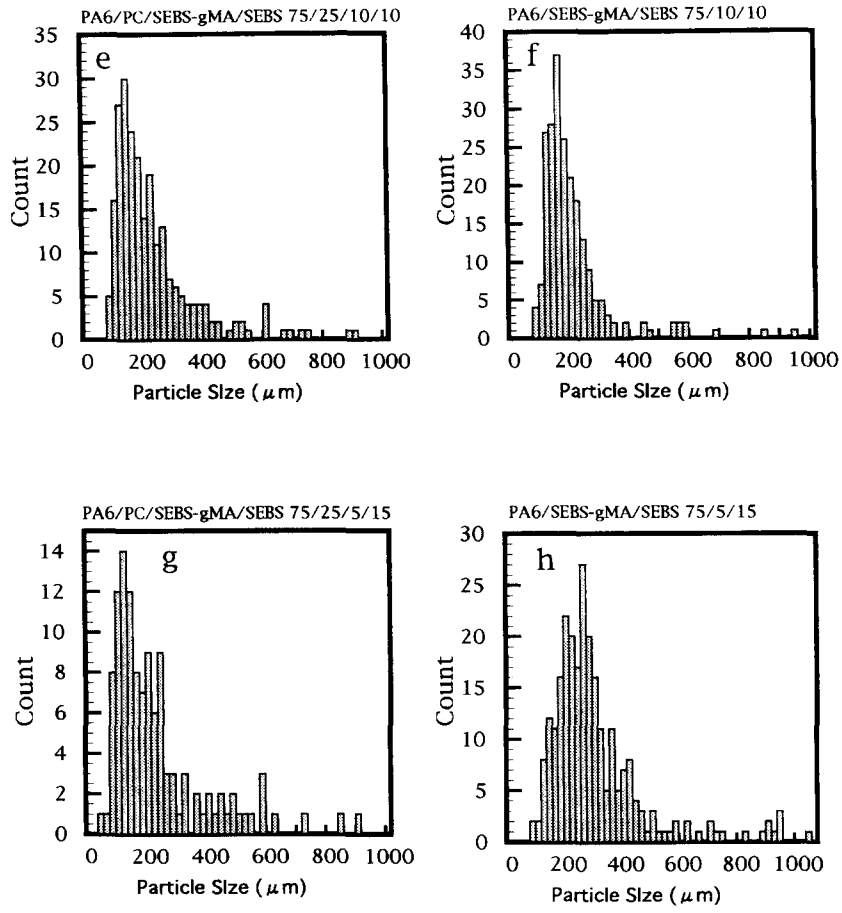

Figure 10 (*Continued*)

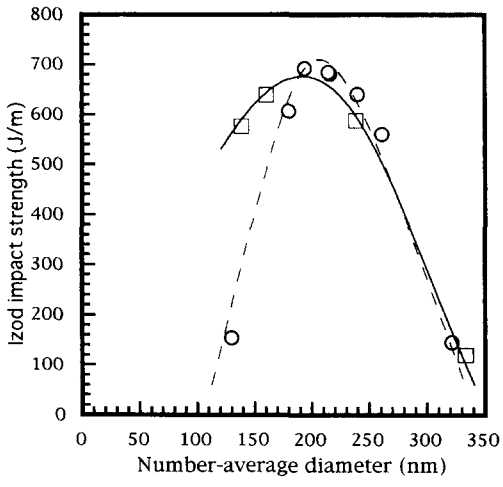

Figure 11 Notched izod impact strength as a function of dispersed SEBS domain size: (○) 75/25 PA6/PC blends; (□) PA6 blends with a combination of SEBS-gMA and SEBS. The ratio of the total amount of SEBS-gMA and unfunctionalized SEBS to PA6 is 20/75 by weight

Through the formation of the microdomain structure on the interface between PA6 and PC, SEBS is expected to work as a thermoplastic elastomer on the domain boundary between PA6 and PC and hence to promote stress distribution and transfer the impact energy to the PC phase. The formation of the SEBS microdomain structure on the domain boundary may toughen the interface sufficiently to compensate for the incompletion of the encapsulation of SEBS on the PC domains. As shown in *Figure 4*, 75/25 PA6/PC blends compatibilized with certain combinations of SEBS-gMA and SEBS to offer a higher impact strength than those obtained from ternary blends of PA6 with combination of SEBS-gMA and SEBS. As mentioned above, the size and distribution of the SEBS domain in the PA6 matrix is almost the same as in the PA6/PC blends compatibilized with the SEBS-gMA/SEBS combination and in the PA6 blends toughened with SEBS-gMA/SEBS. It is thus assumed that in the PA6/PC blends, by introducing the SEBS-gMA/SEBS combination, the domain boundary between PA6 and PC is toughened sufficiently to be able to transfer the impact enery into the PC domains effectively and then the PC domains work as a reinforcing filler.

We also examined the effect of the combination of SEBS-gMA and SEBS on the morphology and impact strength in PC rich blends. The photographs in *Figure 13* compare the morphologies at the same magnification observed in the blends of 25/75 PA6/PC with the combination of 10 phr total SEBS-gMA and SEBS, where PS domains in SEBS are stained with RuO_4. Compared with the PA6-rich blends, morphological changing with the variation of the ratio of SEBS-gMA to SEBS is complicated. In PC-rich blends, SEBS-gMA is occluded in PA6 domains due to the reaction between SEBS and PA6, and it is dispersed in PA6 domains and also exists on the domain boundary between PA6 and PC. By the use of the combination of SEBS-gMA and SEBS, the size of dispersed SEBS domains become larger and the SEBS on the domain boundary become thicker with increasing ratio of unfunctionalized SEBS

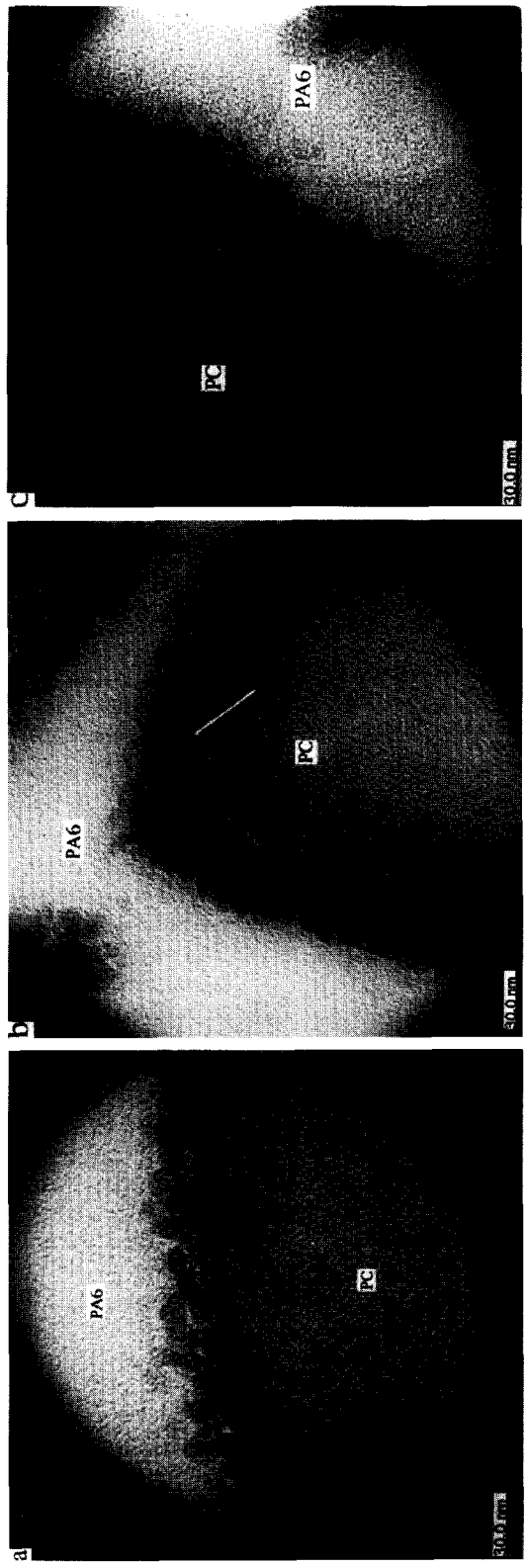

Figure 12 TEM photographs showing the SEBS microdomain structure at the domain boundary between PA6 and PC in the blends of PA6/PC/SEBS-gMA/SEBS: (a) 75/25/20/0, (b) 75/25/19/1 and (c) 75/25/10/10

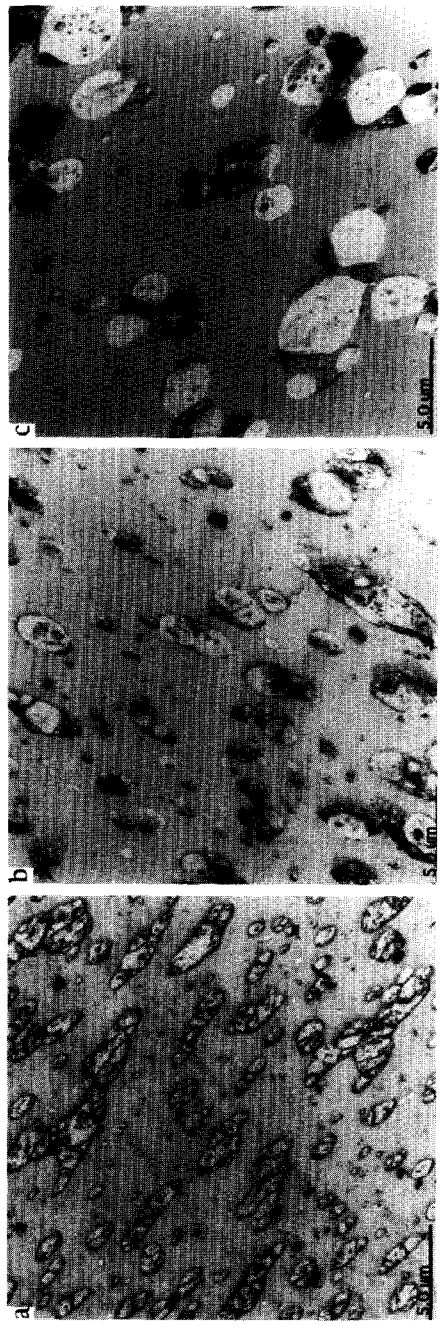

Figure 13 TEM photographs of 25/75 PA6/PC blends compatibilized with SEBS-gMA and unfunctionalized SEBS: (a) 25/75/8/2, (b) 25/75/5/5 and (c) 25/75/2/8 PA6/PC/SEBS-gMA/SEBS blends

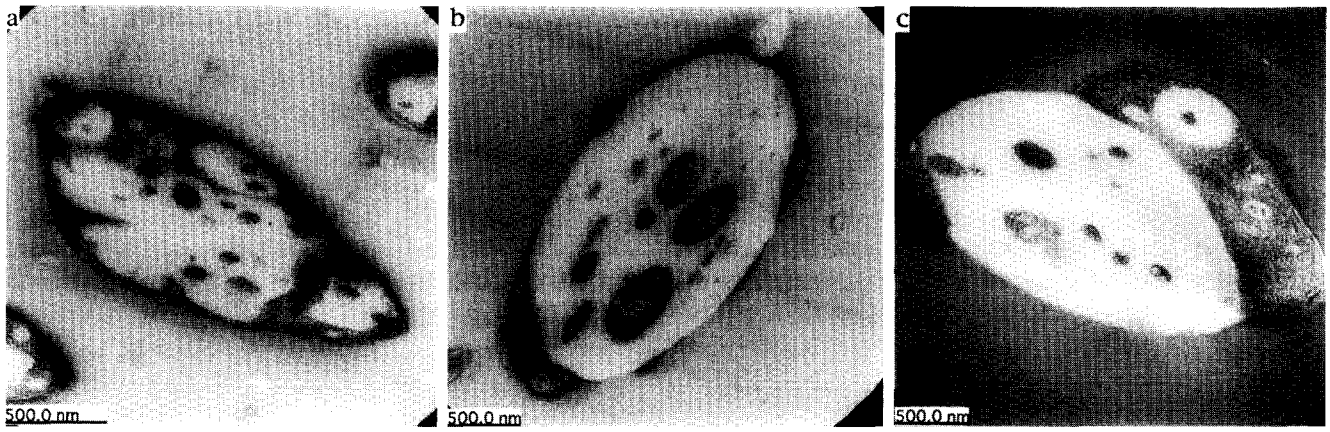

Figure 14 TEM photographs of PA6 domains with occluded SEBS domains in the blends of PA6/PC/SEBS-gMA/SEBS: (a) 25/75/8/2, (b) 25/75/5/5 and (c) 25/75/2/8

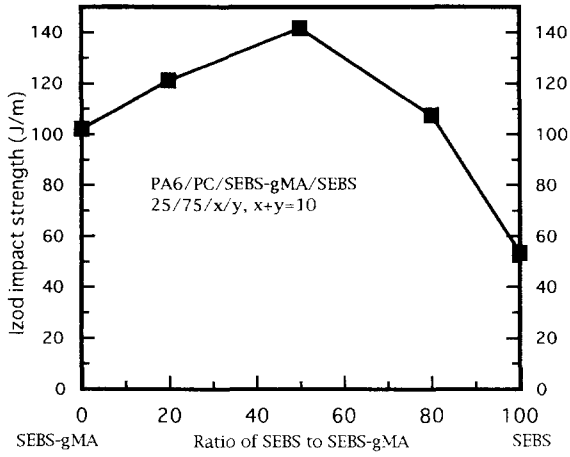

Figure 15 Notched izod impact strength of 27/75 PA6/PC blends as a function of the ratio of SEBS-gMA to SEBS. The added total amount of SEBS-gMA and SEB is 10 phr

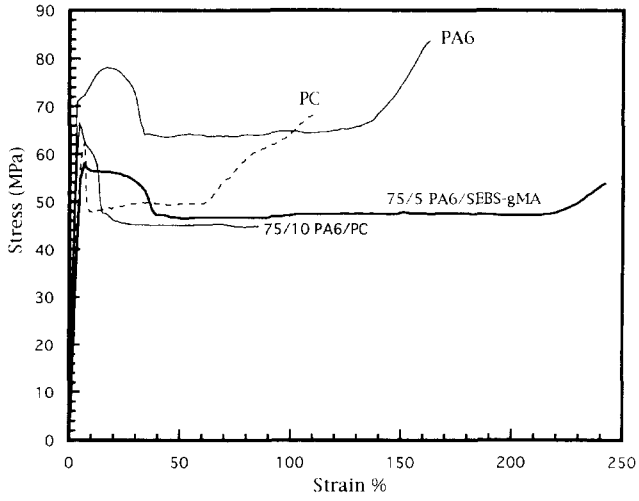

Figure 16 Tensile stress–strain curves of the pure PA6, PC, binary blend of 75/5 PA6/SEBS-gMA and 75/10 PA6/PC

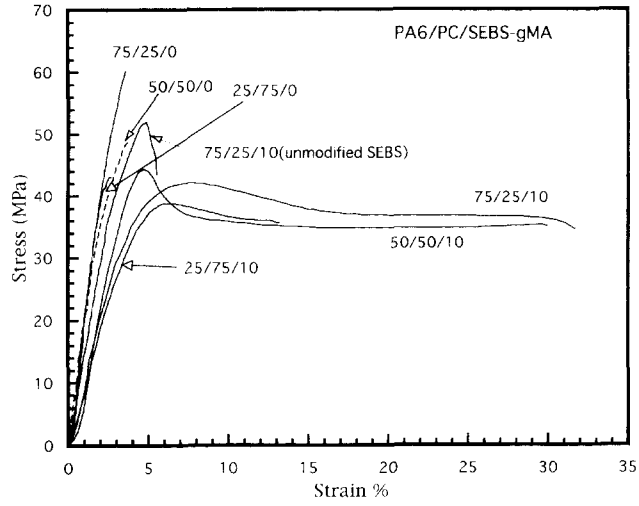

Figure 17 Tensile stress–strain curves of the PA6/PC uncompatibilized blends and compatibilized with SEBS-gMA and with unfunctionalized SEBS

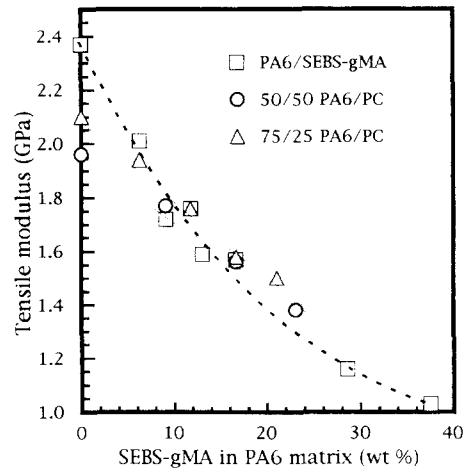

Figure 18 Tensile modulus as a function of the concentration of SEBS-gMA against PA6: (□) binary blends of PA6/SEBS-gMA; (○) 50/50 PA6/PC; (△) 75/25 PA6/PC blends

to SEBS-gMA as shown in *Figure 14*. Additionally the shape and the size of the PA6 domains dispersed in the PC matrix are varied. With SEBS-gMA alone, the PA6 domains show irregular shape. As unfunctionalized SEBS is added, the PA6 domains become spherical. The reason for this is assumed to come from the difference in rheological property in the melt situation. By incorporation of SEBS-gMA into the PA6/PC blend, the viscosity of the PA6 domains in melt situation become greater due to the grafting reaction which

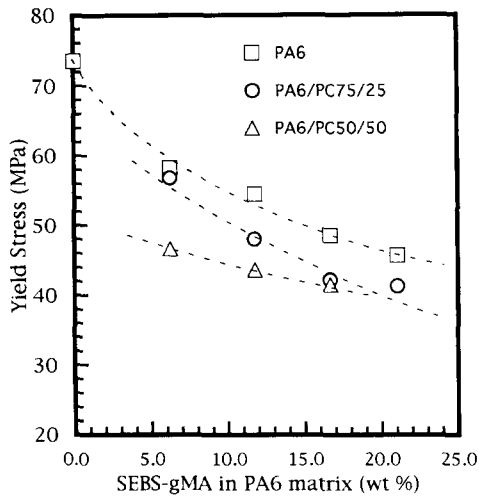

Figure 19 Tensile yield stress as a function of the concentration of incorporated SEBS-gMA in PA6 by weight: (□) binary blends of PA6/SEBS-gMA; (○) 75/25; (△) 50/50 PA6/PC blends with SEBS-gMA

produces higher molecular weight polymers. This may cause the enlargement and also the formation of irregular shaped PA6 domains. As the ratio of unfunctionalized SEBS increases, the extent of the reaction is decreased. This reduces the viscosity of the PA6 domains and as a result the domains tend to be spherical. *Figure 15* shows the effect of the combination of SEBS-gMA and SEBS on the impact strength in 25/75 PA6/PC blends. Each blend contains 10 phr total SEBS-gMA and SEBS,while the ratio of SEBS-gMA to SEBS is varied. As for PA6-rich blends, a certain combination of SEBS-gMA and SEBS offers maximum impact strength. In the case of PC-rich blends, it is difficult to characterize the domain feature quantitatively because many factors in terms of shape and size are involved. Both the shape and the size of PA6 domains accompanying the change of occluded SEBS feature are varied by the variation of the ratio of SEBS-gMA to SEBS. It is, however, obvious qualitatively that, by the use of the combination of SEBS-gMA and SEBS, the SEBS phase on the domain boundary become thicker which may improve interfacial adhesion on the domain boundary and may reduce the stress concentration.

Tensile stress–strain behaviour

Figures 16 and *17* show the typical stress–strain behaviours obtained in this study. The tensile properties obtained from the stress–strain curves are shown in *Tables 1* and *2*. *Figure 16* shows the stress–strain curves of pure PA6 and PC, and also shows the curves of binary blends of PA6/SEBS-gMA (75/5) and PA6/PC (75/10). Both pure polymers exhibit typical stress–strain behaviour of ductile polymers, that is, they show long strain after they yield with necking of specimens, maintaining the same level of stress and, before they break, the stress is rapidly increased. Due to the elastic nature of SEBS, the addition of SEBS-gMA to PA6 decreases the yield strength but increases the elongation at break due to the chemical coupling on the interface between PA6 and SEBS-gMA. The PA6 and PC binary blends, in which the PC content is less than about 10 wt%, show strain after yielding. The yield stress and strain at break, however, are decreased compared to that of pure PA6. As shown in *Figure 17*, the binary blends of 75/25, 50/50 and 25/75 PA6/PC show no yielding and break at a lower stress level, which is characteristic of incompatibilized blends with poor interfacial adhesion. Provided there is no adhesion between the matrix and domains, the domains behave as voids and the tensile strength can be predicted by the following equation[23]:

$$\sigma_v = \sigma_0(1 - 1.2\phi_v^{2/3}) \quad (1)$$

where σ_0 is the tensile strength of matrix and σ_v is the tensile strength of the blend with a volume fraction of ϕ_v assuming that the domains are spherical. Calculations using this equation predict that the tensile strength is 42.72, 14.73 and 38.66 in the 75/25, 50/50 and 25/75 PA6/PC blends, respectively, where ϕ_v is 0.242, 0.511 and 0.242, respectively. In the 50/50 blend, PA6 forms domains and in the others, the minor components form domains. The predicted values are much lower than the experimental ones. This means that even the uncompatibilized blends have some interfacial adhesion on the domain boundary. Compared with the PA6-rich and PC-rich blend, the PC-rich blend (25/75 PA6/PC) shows a closer value to the predicted one. This indicates that the PC-rich blend has poorer adhesion on the domain boundary than the PA6-rich blend. As reported by Gattiglia *et al.*[3], in the PA6 rich blends, the interchange reaction between PA6 and PC during mixing which

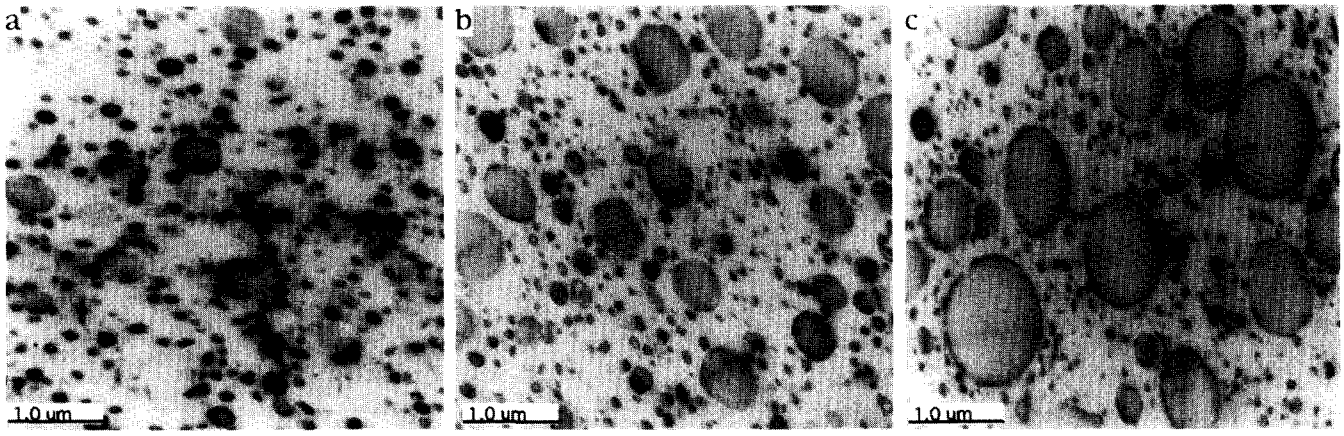

Figure 20 TEM photographs of PA6/PC/SEBS-gMA ternary blends: (a) 75/5/10, (b) 75/15/10 and (c) 75/30/10

Table 4 Interparticle distance and number average diameter of SEBS domains dispersed in the PA6 matrix

Formulation	Interparticle distance distance (nm)	Number average diameter (nm)
PA6/PC/SEBS-gMA		
75/0/10	195	130
75/5/10	206	152
75/15/10	202	138
75/25/10	196	145
75/30/10	186	140
75/0/20	115	138
75/15/20	122	119
75/25/20	120	134
75/35/20	109	147

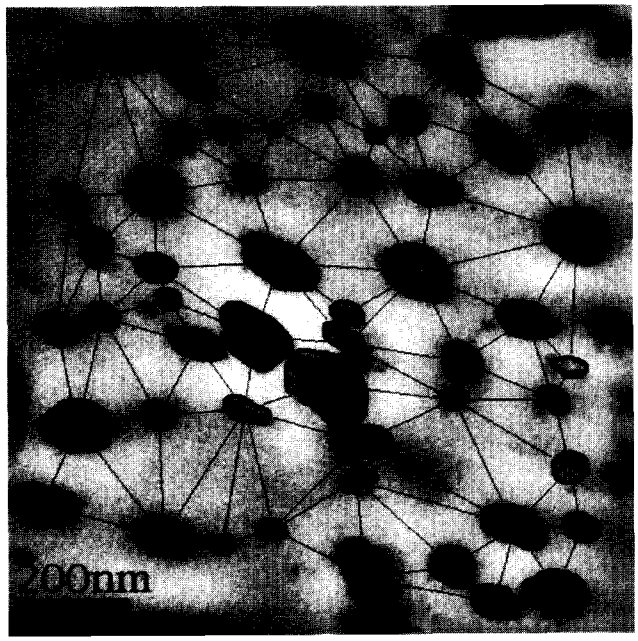

Figure 21 TEM photographs showing SEBS-gMA domains in the blend of 75/35/20 with the results of the measurement of interparticle distance

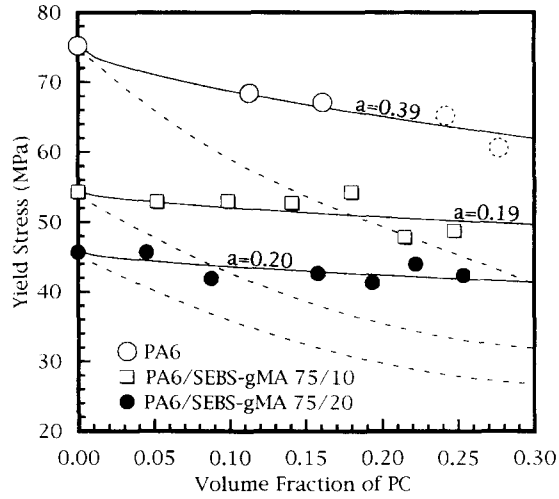

Figure 22 Tensile yield stress and the theoretical predictions based on equations (2) and (3) as a function of the volume fraction of PC: (○) PA6/PC uncompatibilized blends; (□) PA6/PC/SEBS-gMA blends in which the ratio of PA6 to SEBS-gMA is fixed at 75/10 and the PC content is varied: (●) PA6/PC/SEBS-gMA blends in which the ratio of PA6 to SEBS-gMA is fixed at 75/20 and the PC content is varied. The dashed lines represent the predicted value based on equation (2) and the solid lines represent the fitted curves based on equation (3). The stress at break is plotted for the blends showing no yielding instead

produces block copolymer of PA6-PC occurs much more effectively due to a higher concentration of PA6 amine terminals. The formation of PA6-PC copolymer is expected to enhance the compatibility between PA6 and PC. Taking this into account, it is reasonable that PA6-rich blends exhibit better mechanical properties than the PC-rich blends in the uncompatibilized blends, in particular, the blend of 75/10 PA6/PC in which PC is 11 wt% shows yielding and elongation.

As shown in *Figure 17*, the addition of SEBS-gMA improves the tensile properties from brittle to ductile in all compositions evaluated in our study. Although the tensile strength is reduced by the addition of SEBS-gMA, the blends with SEBS-gMA show yielding and elongation with necking of specimens. The blends with unfunctionalized SEBS, on the contrary, show yielding but the strain is too small to show necking. The improvment of tensile properties suggests that the encapsulation of SEBS-gMA around the PC domains contributes to enhancement of interfacial adhesion. The reduction of yield strength from the uncompatibilized blends are assumed to be owing to the elastic nature of SEBS affecting the PA6 matrix. As shown in the TEM photograph in *Figure 3*, SEBS-gMA is dispersed in the PA6 matrix. In addition, the dynamic mechanical analysis reported in our previous paper[14] has revealed that the addition of the SEBS-gMA phase does not influence the glass transition temperature of PC, which indicates that the SEBS-gMA phase does not reside in the PC domains. These results suggest that SEBS-gMA improves the toughness of PA6 but causes a reduction of the tensile modulus and strength. In *Figure 18*, the tensile modulus of the binary blends of PA6/SEBS-gMA and the ternary blends of PA6/PC/SEBS-gMA, in which the compositions of PA6/PC are 75/25 and 50/50, are plotted as a function of the weight fraction of SEBS-gMA in the PA6 matrix. This reveals that the addition of SEBS-gMA to PA6 reduces the tensile modulus of PA6 and that, if the concentration of SEBS-gMA in PA6 matrix is the same, the modulus of the ternary blend, except for uncompatibilized blends, is almost the same as that of the corresponding binary blend and, furthermore, shows a higher value than that at certain levels of the SEBS-gMA loading. The yield strength also shows the same tendency (*Figure 19*), but the ternary blends exhibit slightly lower values than the corresponding binary blends. The reduction of yield strength by the addition of PC to PA6/SEBS-gMA binary blends are discussed below. Nevertheless, the improvement of the tensile properties from brittle to ductile by the addition of SEBS-gMA suggests that the interfacial adhesion on the domain boundary has been improved.

In order to evaluate the interfacial situation on the domain boundary between the PA6 matrix and PC domains, we assume hereafter, regarding the morphological feature of the PA6 rich-ternary blends, that PC domains work as a reinforcing filler for the matrix composed of PA6 and SEBS-gMA. There are two kinds of interface in the PA6/PC/SEBS-gMA blends in which PA6 forms a matrix, one of which is the interface between the PA6 matrix and SEBS-gMA domains and

Table 5 Tensile properties of PA6/PC/SEBS-gMA blends

Formulation	Volume fraction of PC ϕ	Tensile modulus (GPa)	Yield		Break	
			Stress (MPa)	Strain (%)	Stress (MPa)	Strain (%)
PA6/PC/SEBS-gMA						
100/0/0	0	2.37	75.2	3.7	52.4	166.7
75/10/0	0.113	2.13	68.4	4.6	57.9	41.9
75/15/0	0.161	2.07	67.1	5.0	64.2	8.5
75/25/0	0.242	2.10	NI	NI	65.2	4.4
75/30/0	0.277	2.05	NI	NI	60.6	3.7
50/50/0	0.489	1.96	NI	NI	41.5	2.4
75/0/10	0	1.76	54.5	5.3	46.8	200.0
75/5/10	0.052	1.86	52.9	6.7	53.6	188.5
75/10/10	0.099	2.02	53.0	4.5	46.1	114.6
75/15/10	0.141	2.00	52.7	4.5	38.9	65.3
75/20/10	0.180	2.03	54.3	5.0	55.9	108.1
75/25/10	0.215	2.04	48.0	3.8	35.9	31.3
75/30/10	0.248	2.06	48.7	4.7	42.9	101.6
75/0/20	0	1.52	45.7	14.9	45.6	260.3
75/5/20	0.046	1.61	45.7	10.8	50.4	219.1
75/10/20	0.088	1.54	41.9	16.3	38.7	182.3
75/20/20	0.161	1.51	42.7	9.9	41.1	61.5
75/25/20	0.194	1.50	41.3	4.7	33.7	59.2
75/30/20	0.224	1.67	43.8	9.4	42.2	75.4
75/35/20	0.252	1.60	42.5	9.4	28.8	51.6

NI: Not identified

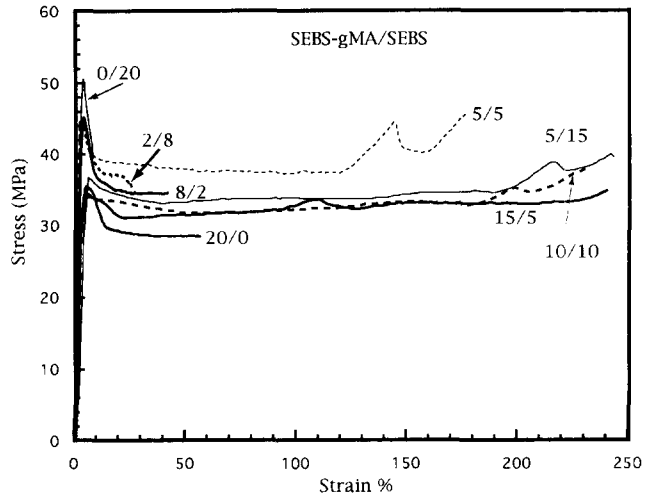

Figure 23 Tensile stress–strain curves showing the large strain obtained by the use of a combination of SEBS-gMA and SEBS in 75/25 PA6/PC blends

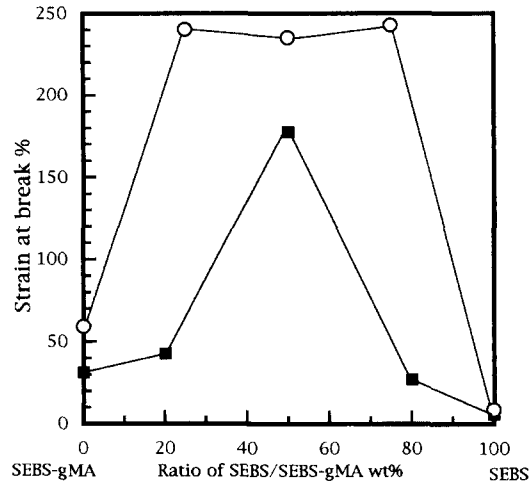

Figure 24 Tensile strain at break as a function of the ratio of SEBS-gMA to unfunctionalized SEBS in 75/25 PA6/PC blends: (■) total amount of SEBS is 10 phr and (○) 20 phr

the other is that between PC domains and SEBS-gMA encapsulating the PC domains. It is reasonable to suppose that the former interface is bonded more strongly than the latter, because the PA6 matrix bonds with SEBS-gMA domains by chemical coupling whilst the PC domains contact the SEBS-gMA only by physical interaction.

It is well known that the interfacial characteristics play an important role in tensile properties of multiphase blends. The discontinuities in stress transfer at the interface of dispersed phase and matrix cause the increase of stress concentration at the interface and hence leads to poor tensile properties of the blends. If there is perfect adhesion between the phases, the stress transfer across the interfaces is continuous and, in the absence of any adhesion, the blend would behave as if the matrix is embedded with holes, causing complete discontinuity in stress transfer or stress concentration at the interface. In the PA6/PC/SEBS-gMA blends, the interface between PC domains and SEBS-gMA encapsulating them is expected to be the stress concentration site because of its relative adhesion weakness compared with the adhesion between PA6 and SEBS-gMA. The

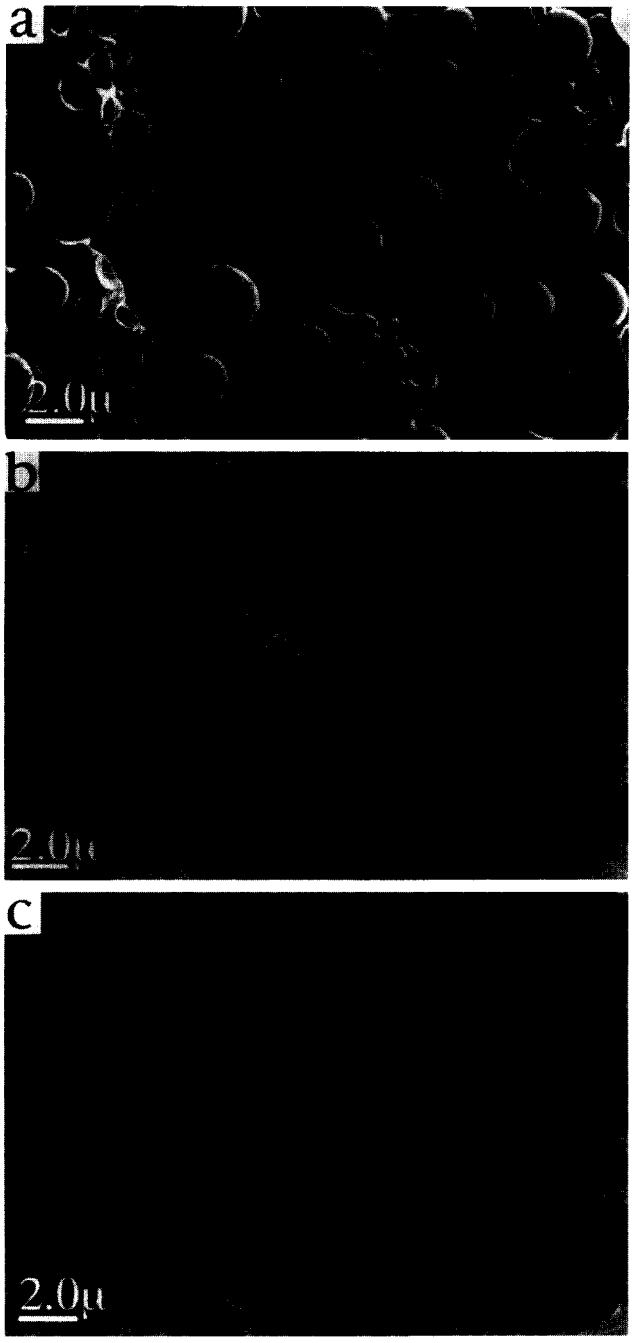

Figure 25 SEM photographs of tensile fracture surfaces of 75/25 PA6/PC blends: (a) uncompatibilized; (b) compatibilized with 20 phr SEBS-gMA; (c) compatibilized with a combination of 10/10 SEBS-gMA/unfunctionalized SEBS

stronger the adhesion between PC and SEBS-gMA, the better the tensile properties achieved.

First, we analyse yield stress data representing the small deformation properties using the simple theory proposed by Nielsen[24] for the variation of tensile yield strength with blend composition given as:

$$\epsilon_b = \epsilon_m(1 - \phi_d^{2/3}) \quad (2)$$

where ϵ_b and ϵ_m are yield strength of the blend and the matrix, respectively, and ϕ_d is the volume fraction of the inclusions. This equation indicates that the yield strength of incompatible blends decreases with increasing volume fraction of a dispersed phase. We evaluate the stress

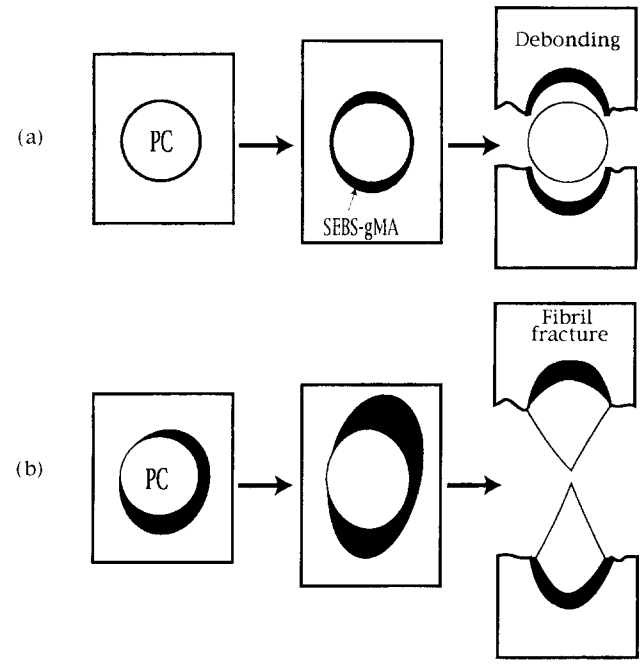

Figure 26 Schematic illustration of fracture mode of PA6/PC blends compatibilized with: (a) SEBS-gMA alone and (b) a combination of SEBS-gMA and SEBS

concentration effect at an interface as evaluated by Srinivasan and Gupta *et al.*[25] for the PP/SEBS/PC ternary blends. They introduced a parameter a to equation (1) as a multiplication factor in the second term as follows:

$$\epsilon_b = \epsilon_m(1 - a\phi_d^{2/3}) \quad (3)$$

If the parameter a has a low positive value, the inclusion would have little effect on the yield stress of the blend, indicating that the stress concentration at the interface is low and hence the interfacial adhesion would be good. In fact, Nicolais and Narkis modified equation (1) for composite systems lacking interfacial adhesion by changing the multiplication factor for $\phi_d^{2/3}$ from 1 to 1.21 as follows[26]:

$$\epsilon_b = \epsilon_m(1 - 1.21\phi_d^{2/3}) \quad (4)$$

We investigated the effect of the incorporation of PC to PA6/SEBS-gMA on the yield stress by varying the fraction of PC in the PA6/SEBS-gMA matrix of which compositions are fixed at 75/0, 75/10 and 75/20. *Figure 20* shows the TEM photographs of the 75/10/10, 75/20/10 and 75/30/10 PA6/PC/SEBS-gMA blends. These photographs indicate that the dispersion of SEBS-gMA in the PA6 matrix is independent of the PC content when the composition of PA6/SEBS-gMA is the same, whereas the size of the PC domains are increased with increasing amounts of PC. Quantitatively, the average size of domains and the distance between the neighbouring domains are almost the same as summarized in *Table 4*. Interparticle distances defined by Wu[27] between the neighbouring SEBS domains were obtained using image analysis of TEM photographs. The one example is shown in *Figure 21*. This situation enables us to analyse the yield stress with equation (3) by considering PA6/SEBS-gMA as the matrix and PC as the inclusion. *Table 5* summarizes the tensile properties for this blend series.

In *Figure 22*, the yield stress is plotted against the volume fraction of PC. As mentioned above, uncompatibilized blends of PA6/PC in which PC comprises less than 10 wt% show yields but, with increase of PC fraction, the blends show no yield points and change to a brittle nature. For the blends which show brittleness, stress at break is plotted there instead. Then, the parameter a in equation (3) is determined by fitting the experimental data as shown in *Figure 22*. The theoretical values predicted by equation (2) are also plotted in *Figure 22* as dashed lines. This shows that the experimental values are all greater than the predicted values from equation (2), implying that even the uncompatibilized blends have some interfacial adhesion to reduce the stress concentration at the interface. The value of a obtained by fitting of experimental results for each blend series is 0.39, 0.19 and 0.21 for uncompatibilized, 75/10 and 75/20 PA6/PC, respectively. The reduction of a from 0.39 to 0.19 implies a decrease of stress concentration effect by the addition of SEBS-gMA. Although the value of a is slightly increased from 0.19 to 0.21 when the incorporation of SEBS-gMA is increased, this may be within experimental error and hence this means that the further addition of SEBS-gMA cannot decrease the stress concentration effect. In fact, analysis of the interfacial situation by TEM reveals that the encapsulation of SEBS-gMA on the PC domains is achieved by the addition of 5 phr SEBS-gMC and then the encapsulation situation is unchanged by the further addition of SEBS-gMA. Analysis of the yield stress data by introducing the simple theory provides evidence that the incorporation of SEBS-gMA to PA6/PC blends reduces the stress concentration effect at the domain boundary between PA6 and PC. However, we have not yet obtained direct evidence for the improvement of interfacial adhesion through the encapsulation of SEBS-gMA around the PC domains.

Next, the data for strain at break as a large deformation property are analysed. It is well known that the strain at break is very sensitive to the interfacial situation. To achieve a high fracture strain with multiphase blends, the domains have to be deformed under the strain of the matrix. In order for that, strong interfacial adhesion on the domain boundary is essential. To achieve high fracture strain, the interfacial adhesion has to be strong enough to prevent domain debonding before yielding. Therefore, the interfacial adhesion between the PC domains and PA6 matrix compatibilized with SEBS-gMA is speculated to be above the yield stress of them. In the uncompatibilized blends, on the other hand the interfacial strength is less then the yield stress and debonding occurs before yielding. Compared to the long fracture strain obtained in the pure PA6 and PC, the fracture strain of the ternary blends of PA6/PC/SEBS-gMA is still low. This means that the interfacial adhesion between PA6 and PC is insufficient and hence debonding between the PC domains and PA6 matrix occurs during the strain. In other words, under large deformation of the PA6/SEBS-gMA matrix, the interfacial strength becomes poor and then the stress transfer becomes less effective, hence the PC domains cannot follow the deformation of the matrix, resulting in the debonding.

Figure 23 shows the stress–strain curves of 75/25 PA6/PC blends compatibilized with combinations of SEBS-gMA and SEBS. This shows that a significantly higher fracture strain can be achieved by the use of a combination of SEBS-gMA and SEBS, while the stress is kept at the same level among the blends with the same amount of total SEBS-gMA and SEBS. *Figure 24* shows the plots of three fracture strain vs the ratio of SEBS-gMA to SEBS. As obtained in the results of notched izod impact strength, the fracture strain also shows the same tendency that the maximum value can be obtained by the use of a certain combination of SEBS-gMA and SEBS. The fracture is comparable to that of the pure PA6 and is moreover, higher than that. This significant increase of fracture strain implies a change of fracture mode. *Figure 25* shows SEM photographs showing the fracture surfaces after tensile tests of the 75/25 PA6/PC blends uncompatibilized, compatibilized with 20 phr SEBS-gMA and with the combination of 10/10 SEBS-gMA/SEBS. The uncompatibilized blend of 75/25 PA6/PC shows that the undeformed PC particles debonded from PA6 matrix with a smooth fracture surface (*Figure 25a*). The fracture surface of 75/25/20 PA6/PC/SEBS-gMA shows that the PA6 matrix is drawn out and fibrillated but the PC domains remain undeformed (*Figure 25b*). In the 75/25/10/10 PA6/PC/SEBS-gMA/SEBS blend, most of the components are fibrillated while some undeformed PC particles are observed, suggesting that some of the PC domains are fractured rather than debonded during final separation (*Figure 25c*). These results indicate that the fracture mode progressed from debonding to partial drawing and fibril fracture by the use of a proper combination of SEBS-gMA and SEBS. With regard to the elastic property of SEBS, it is inferred that the SEBS on the domain boundary is deformed during the strain and thus dissipates the strain energy. In the blends compatibilized with SEBS-gMA alone, the dissipation of strain energy is insufficient and hence debonding occurs. On the other hand, in the blends compatibilized with SEBS-gMA/SEBS combination, the SEBS phase encapsulating the PC domains are thick enough to deform significantly and to dissipate the energy effectively. *Figure 26* illustrates schematically the fracture modes mentioned above. In the 75/25 PA6/PC blends with SEBS-gMA alone, SEBS-gMA surrounding the PC domains are deformed but the debonding occurs due to the small deformation. By the use of the combination of SEBS-gMA and SEBS, the SEBS phase on the domain boundary is thick enough to deform significantly and PC domains are also fibrillated. In the 75/25 PA6/PC blends compatibilized with a combination of SEBS-gMA and SEBS, a peak in the stress–strain curve during the strain before they break can be detected as shown in *Figure 23*. It may be inferred that the highly oriented PC molecules are generated during the large strain and then the PC domains fracture before the specimen is separated. As mentioned above, the size of PC domains is almost constant with the variation of the ratio of SEBS-gMA to SEBS. This suggests that the major contribution of the increase of interfacial adhesion is from the phase situation of SEBS encapsulating the PC domains in PA6 matrix.

CONCLUSIONS

This paper described that, through the reaction induced phase formation in the ternary blends of

PA6/PC/SEBS-gMA, the adhesion on the domain boundary between PC and PA6 has been improved, which leads to an improvement in mechanical properties. In the blends where PA6 forms the matrix, SEBS-gMA encapsulates the dispersed PC domains in the PA6 matrix and in addition SEBS-gMA is dispersed finely in the PA6 matrix. Through this phase formation, SEBS-gMA works as an impact modifier for the PA6 matrix and at the same time works as a coupling agent for the adhesion of the PA6 matrix and PC domains. In the PC-rich blends, SEBS-gMA is occluded in the PA6 domains where some SEBS-gMA is dispersed in the PA6 domains and some exists on the domain boundary between the PC matrix and PA6 domains. This phase formation also improves the mechanical properties. In the PA6-rich blends, when the composition of PA6/PC is fixed, the average size of the dispersed PC domains is constant with the variation of this incorporation of SEBS-gMA and SEBS. This fortunately simplifies the relationship between the morphology and mechanical properties, reducing the number of factors to be taken into consideration. Namely, the size of the dispersed SEBS domain in the PA6 matrix and the situation of the encapsulation by SEBS-gMA around the PC domains are major factors affecting the mechanical properties. On the other hand, the PC-rich blends show relatively complicated morphological variation with the variation of the amount and combination of SEBS-gMA and SEBS.

We demonstrated that the use of the combination of SEBS-gMA and SEBS as a compatibilizer for PA6/PC blends is an effective way to achieve maximum mechanical properties. In the blends where PC domains are dispersed in the PA6 matrix, it is of interest that the encapsulation of SEBS around the PC domains gradually becomes incomplete with an increase in the unfunctionalized SEBS ratio against SEBS-gMA. It is generally recognized that the incomplete encapsulation leads to stress concentration and hence results in poor mechanical properties. In our case, however, the results are absolutely contrary to the normal acceptance. Both the results of the notched izod impact strength and tensile properties suggest that the interfacial strength is much higher with the combination of SEBS-gMA and SEBS than with SEBS-gMA alone. As the ratio of unfunctionalized SEBS is increased, the SEBS phase becomes gradually thicker accompanied by incomplete encapsulation. The thick SEBS phase on the domain boundary contains original microdomain structure between the PA6 matrix and the PC domain. We assume that the original microdomain structure of SEBS functions as a thermoplastic elastomer on the domain boundary which enhances the stress dissipation and reduce the stress concentration on the domain boundary effectively enough to compensate for the incomplete encapsulation. In other words, the domain boundary is toughened. The detailed analysis of the deformed area will reveal the mechanism for this remarkable improvement in the mechanical properties.

REFERENCES

1 Gattiglia, E., Turturro, A. and Pedemonte, E. *J. Appl. Polym. Sci.* 1989, **38,** 1807
2 Gattiglia, E., Turturro, A., Pedemonte, E. and Dondero, G. *J. Appl. Polym. Sci.* 1990, **41,** 1411
3 Gattiglia, E., Turturro, A., La Mantia, E. P. and Velenza, A. *J. Appl. Polym. Sci.* 1992, **46,** 1887
4 Valenza, A., La Manta, E. P., Gattilglia, E. and Turturro, A. *Int. Polym. Process* 1994, **6,** 3
5 Majumdar, B., Keskkula, H., Paul, D. R. and Harrey, N. G. *Polymer* 1994, **35,** 4263
6 Triacca, V. J., Ziaee, S., Barlow, W. J., Keskkula, H. and Paul, D. R. *Polymer* 1991, **32,** 1401
7 Majumdar, B., Keskkula, H. and Paul, D. R. *Polymer* 1994, **35,** 5453
8 Majumdar, B., Keskkula, H. and Paul, D. R. *Polymer* 1994, **35,** 5468
9 Duvall, J., Selliti, C., Myers, C., Hiltner, A. and Baer, E. *J. Appl. Polym. Sci.* 1994, **52,** 195
10 Duval, J., Selliti, C., Topolkaraev, V., Hiltner, A., Baer, E. and Myers, C. *Polymer* 1994, **35,** 3948
11 Tang, T., Li, H. and Huang, F. C. *Macromol. Chem. Phys.* 1994, **195,** 2931
12 Lee, P. C., Kuo, W. F. and Chang, F. C. *Polymer* 1994, **35,** 5641
13 Molsti-Miettinen, R. M., Heino, M. T. and Seppala, J. V. *J. Appl. Polym. Sci.* 1995, **57,** 573
14 Horiuchi, S., Macthariyakul, N., Yase, K., Kitano, T., Choi, H. K. and Lee, Y. M. *Polymer* 1996, **37,** 3065
15 Bauer, R. in 'Methods in Microbiology' (Ed. F. Mayer), Academic Press, London, 1988, p. 113
16 Reimer, L. in 'Energy Filtering Transmission Electron Microscopy' (Ed. L. Reimer), Springer, Heidelberg, 1995, p. 347
17 Oshinksi, A. J., Keskkula, H. and Paul, D. R. *Polymer* 1992, **33,** 268
18 Oshinksi, A. J., Keskkula, H. and Paul, D. R. *Polymer* 1992, **33,** 284
19 Takeda, Y., Kesskula, H. and Paul, D. R. *Polymer* 1992, **33,** 3173
20 Majumdar, B., Keskkula, H. and Paul, D. R. *Polymer* 1994, **35,** 1386
21 Majumdar, B., Keskkula, H. and Paul, D. R. *Polymer* 1994, **35,** 1399
22 Majumdar, B., Keskkula, H. and Paul, D. R. *J. Appl. Polym. Sci.* 1994, **54,** 339
23 Ishai, O. and Cohen, L. J. *J. Comp. Mater.* 1968, **2,** 302
24 Nielsen, L. E. *J. Appl. Polym. Sci.* 1966, **10,** 97
25 Srinivasan, K. R. and Gupta, A. K. *J. Appl. Polym. Sci.* 1994, **53,** 1
26 Nicolais, L. and Narkis, M. *Polym. Eng. Sci.* 1971, **11,** 194
27 Wu, S. *Polymer* 1985, **26,** 1855